



## Combined Upper Limits on Standard-Model Higgs-Boson Production from the DØ Experiment

The DØ Collaboration  
URL <http://www-d0.fnal.gov>  
(Dated: April 11, 2007)

Upper limits on the cross section for Standard Model Higgs-boson production in  $p\bar{p} \rightarrow H + X$  at  $\sqrt{s} = 1.96$  TeV are determined for  $100 < m_H < 200$  GeV/ $c^2$ . The contributing production processes include associated production ( $WH \rightarrow \ell\nu b\bar{b}$ ,  $ZH \rightarrow \ell\ell/\nu\nu b\bar{b}$ ) and gluon fusion ( $H \rightarrow W^+W^-$ ). Analyses are conducted with integrated luminosities from  $0.84 \text{ fb}^{-1}$  to  $1.05 \text{ fb}^{-1}$  recorded by the DØ experiment. Limits for various combinations of the channels are presented. The results are in good agreement with background expectations and the 95% CL upper limits are found to be a factor of 8.4 (3.7) higher than the Standard Model cross section at  $m_H = 115$  (160) GeV/ $c^2$ .

*Preliminary Results for Winter 2007 Conferences*

TABLE I: List of analysis channels, corresponding integrated luminosities, and final variables. See the Introduction for details.

Channel	Luminosity (fb <sup>-1</sup> )	Final Variable	Reference
$WH \rightarrow e\nu b\bar{b}$ , ST/DT	0.97	Dijet mass	[4]
$WH \rightarrow \mu\nu b\bar{b}$ , ST/DT	1.05	Dijet mass	[4]
$WH \rightarrow \ell\nu b\bar{b}$ , DT	0.93	Dijet mass	[5]
$ZH \rightarrow \nu\bar{\nu} b\bar{b}$ , DT	0.93	Dijet mass	[5]
$ZH \rightarrow \mu^+\mu^- b\bar{b}$ , DT	0.84	Dijet mass	[6]
$ZH \rightarrow e^+e^- b\bar{b}$ , DT	0.92	Dijet mass	[6]
$H \rightarrow W^+W^- (e^+e^-)$	0.95	$\Delta\varphi(e^+, e^-)$	[7]
$H \rightarrow W^+W^- (e^\pm\mu^\mp)$	0.95	$\Delta\varphi(e^\pm, \mu^\mp)$	[7]
$H \rightarrow W^+W^- (\mu^+\mu^-)$	0.95	$\Delta\varphi(\mu^+, \mu^-)$	[8]

## I. INTRODUCTION

Despite its success as a predictive tool, the Standard-Model (SM) of particle physics remains incomplete without a means to explain electroweak-symmetry breaking. The simplest proposed mechanism involves the introduction of a complex doublet of scalar fields that generate particle masses via their mutual interactions. After accounting for longitudinal polarizations in the electroweak sector, this so-called Higgs mechanism also gives rise to a single scalar boson with an unpredicted mass. Direct searches in  $e^+e^- \rightarrow Z^* \rightarrow ZH$  at the Large Electron Positron (LEP) collider yielded lower mass limits at  $m_H > 114.4$  GeV/c<sup>2</sup>[1] while indirect constraints favor  $m_H < 144$  GeV/c<sup>2</sup>[2], with both limits set at 95% CL. The SM Higgs boson search is one of the main goals of the Fermilab Tevatron physics program.

In this note, we combine recent results for direct searches for SM Higgs bosons in  $p\bar{p}$  collisions at  $\sqrt{s} = 1.96$  TeV and recorded by the DØ experiment[3]. These are searches for Higgs bosons produced in association with vector bosons ( $p\bar{p} \rightarrow W/ZH \rightarrow \ell\nu/\ell\ell/\nu\nu b\bar{b}$ ) or singly through gluon-gluon fusion ( $p\bar{p} \rightarrow H \rightarrow W^+W^-$ ). The searches were conducted with data collected during the period 2002-2006 and correspond to integrated luminosities ranging from 0.84 fb<sup>-1</sup> to 1.05 fb<sup>-1</sup>. The searches are separated into eleven final states, referred to as analyses in the following. Each analysis is designed to isolate a particular final state defined by a Higgs boson production and decay mode. In order to ensure proper combination of signals, the analyses were designed to be mutually exclusive after analysis selections.

The eleven analyses[4–8] are categorized by their production processes and outlined in Table I. In the cases of  $p\bar{p} \rightarrow W/ZH$  production, we search for a Higgs-boson decaying to two bottom-quarks. For the  $p\bar{p} \rightarrow WH \rightarrow \ell\nu b\bar{b}$  decays, the analyses are separated into two orthogonal groups: one in which two of the  $b$ -quarks were tagged via  $b$ -jet identification or  $b$ -tagging (herein called double-tag or DT) and one group in which only one  $b$ -quark was tagged (single-tag or ST). In these analyses, only final states with exactly two jets are selected. For the  $ZH \rightarrow \ell\ell/\nu\nu b\bar{b}$  analyses, only the double-tag is considered and two or more jets are required in the final state. The decays of the vector bosons further define the analyzed final states:  $WH \rightarrow e\nu b\bar{b}$ ,  $WH \rightarrow \mu\nu b\bar{b}$ ,  $ZH \rightarrow \ell\ell b\bar{b}$ , and  $ZH \rightarrow \nu\bar{\nu} b\bar{b}$ . In the case of  $WH \rightarrow \ell\nu b\bar{b}$  production, the primary lepton from the  $W$ -boson decay may fall outside of the detector fiducial volume or is not reconstructible. This case is treated as a separate  $WH$  analysis, to which we refer as  $WH \rightarrow \ell\nu b\bar{b}$ . For this channel, the background is the same as the  $ZH \rightarrow \nu\bar{\nu} b\bar{b}$  analysis. In the case of  $p\bar{p} \rightarrow H \rightarrow W^+W^-$  production, we again search for leptonic  $W$  boson decays with three final states:  $WW \rightarrow e^+\nu e^-\nu$ ,  $e^\pm\nu\mu^\mp\nu$ , and  $\mu^+\nu\mu^-\nu$ . For the gluon fusion process,  $H \rightarrow b\bar{b}$  decays are not considered due to the large multijets background.

All Higgs signals are simulated using PYTHIA v6.202[9] using CTEQ6L1[10] leading order parton distribution functions. The signal cross sections are normalized to next-to-next-to-leading order calculations[11, 12] and branching ratios are calculated using HDECAY[13]. The contributions from multijet backgrounds (QCD production) are measured in data. The other backgrounds were generated by PYTHIA, ALPGEN[14], and COMPHEP[15], with PYTHIA providing parton-showering and hadronization. Background cross sections are either normalized to next-to-leading order calculations from MCFM[16] or to data control samples.

## II. LIMIT CALCULATIONS

We combine results using the  $CL_s$  method with a log-likelihood ratio (LLR) test statistic[17]. The value of  $CL_s$  is defined as  $CL_s = CL_{s+b}/CL_b$  where  $CL_{s+b}$  and  $CL_b$  are the confidence levels for the signal plus background hypothesis and the background-only (null) hypothesis, respectively. These confidence levels are evaluated by integrating corresponding LLR distributions populated by simulating outcomes via Poisson statistics. Separate channels and bins

are combined by summing LLR values per channel, per bin. This method provides a robust means of combining individual channels while incorporating systematic uncertainties. Systematics are treated as uncertainties on the expected numbers of signal and background events, not the outcomes of the limit calculations. This approach ensures that the uncertainties and their correlations are propagated to the outcome with their proper weights. The  $CL_s$  approach used here utilizes binned final-variable distributions rather than a single-bin (fully-integrated) value.

### A. Final Variable Preparation

In the case of the  $H \rightarrow b\bar{b}$  analyses, the final variable used for limit setting is the invariant dijet mass, in both the ST and DT selections. Examples of these types of distributions are shown in Figs 1a-d. In the  $H \rightarrow W^+W^-$  analyses, the Higgs mass cannot be directly reconstructed due to the neutrinos in the final state. Thus, the  $p\bar{p} \rightarrow H \rightarrow W^+W^-$  analyses use the difference in the azimuthal angle ( $\varphi$ ) between the two final state leptons ( $\Delta\varphi(\ell_1, \ell_2)$ ), as shown in Fig. 1e. Each signal and background final variable is smoothed via Gaussian kernel estimation[18] to minimize any statistical fluctuation in the shape of the final variable.

To decrease the granularity of the steps between simulated Higgs masses in the limit calculation, additional Higgs mass points are created via signal point interpolation[19]. The primary motivation of this procedure is to provide a means of combining analyses which do not share a common simulated Higgs mass. However, this procedure also allows a measurement of the behavior of each limit on a finer granularity than otherwise possible.

### B. Systematic Uncertainties

The systematic uncertainties differ between analyses for both the signals and backgrounds[4–8]. Here we will summarize only the largest contributions. All analyses carry an uncertainty on the integrated luminosity of 6.5%. The  $H \rightarrow b\bar{b}$  analyses have an uncertainty on the  $b$ -tagging rate of 4-6% per tagged jet. These analyses also have an uncertainty on the jet measurement and acceptances of  $\sim 7.5\%$ . For the  $H \rightarrow W^+W^-$  analyses, the largest uncertainties are those associated with lepton measurement and acceptances. These values range from 3-6% depending on the final state. The largest contributing factors for all analyses is the uncertainty on the background cross sections at 6-18% depending on the background. The uncertainty on the expected multijet background is dominated by the statistics of the data sample from which it is estimated, and is considered separately from the other cross section uncertainties. More complete details for systematic uncertainties are given in Table II.

The systematic uncertainties for the background rates are generally several times larger than the signal expectation itself and are thus an important factor in the calculation of limits. As such, each systematic uncertainty is folded into the signal and background expectations in the limit calculation via Gaussian distribution. These Gaussian values are sampled for each Poisson MC trial (pseudo-experiment). Correlations between systematic sources are carried through in the calculation. For example, the uncertainty on the integrated luminosity is held to be correlated between all signals and backgrounds and, thus, the same fluctuation in the luminosity is common to all channels for a single MC trial. All systematic uncertainties originating from a common source are held to be correlated, as detailed in Tables II and III.

To ameliorate the degrading effects of systematics on search sensitivity, the background fractions are fitted to the data observation by minimizing a profile likelihood[20]. The fit computes the optimal central values for the systematic uncertainties, while accounting for departures from the nominal prediction. A fit is performed separately for the background-only and signal-plus-background hypotheses for each Poisson MC trial.

## III. DERIVED UPPER LIMITS

We derive limits on SM Higgs boson production  $\sigma \times BR(H \rightarrow b\bar{b}/W^+W^-)$  via eleven individual analyses[4–8]. These analyses are first grouped by final state to produce individual results. We group channels by production modes to form combined results. The limits are derived at a confidence level (CL) of 95%. To facilitate model transparency and to accommodate analyses with different degrees of sensitivity, we present our results in terms of the ratio of 95% CL upper cross section limits to the SM cross sections ( $\sigma \times BR(H \rightarrow X)$ ) as a function of Higgs mass. The SM prediction for Higgs boson production would therefore be considered excluded at 95% CL when this limit ratio falls below unity. As described earlier, the  $WH \rightarrow \ell\nu b\bar{b}$  and  $ZH \rightarrow \nu\bar{\nu} b\bar{b}$  channels contribute to the  $WH$  and  $ZH$  limits, respectively. For the fully combined limit, the  $WH \rightarrow \ell\nu b\bar{b}$  and  $ZH \rightarrow \nu\bar{\nu} b\bar{b}$  signals are summed with one common background.

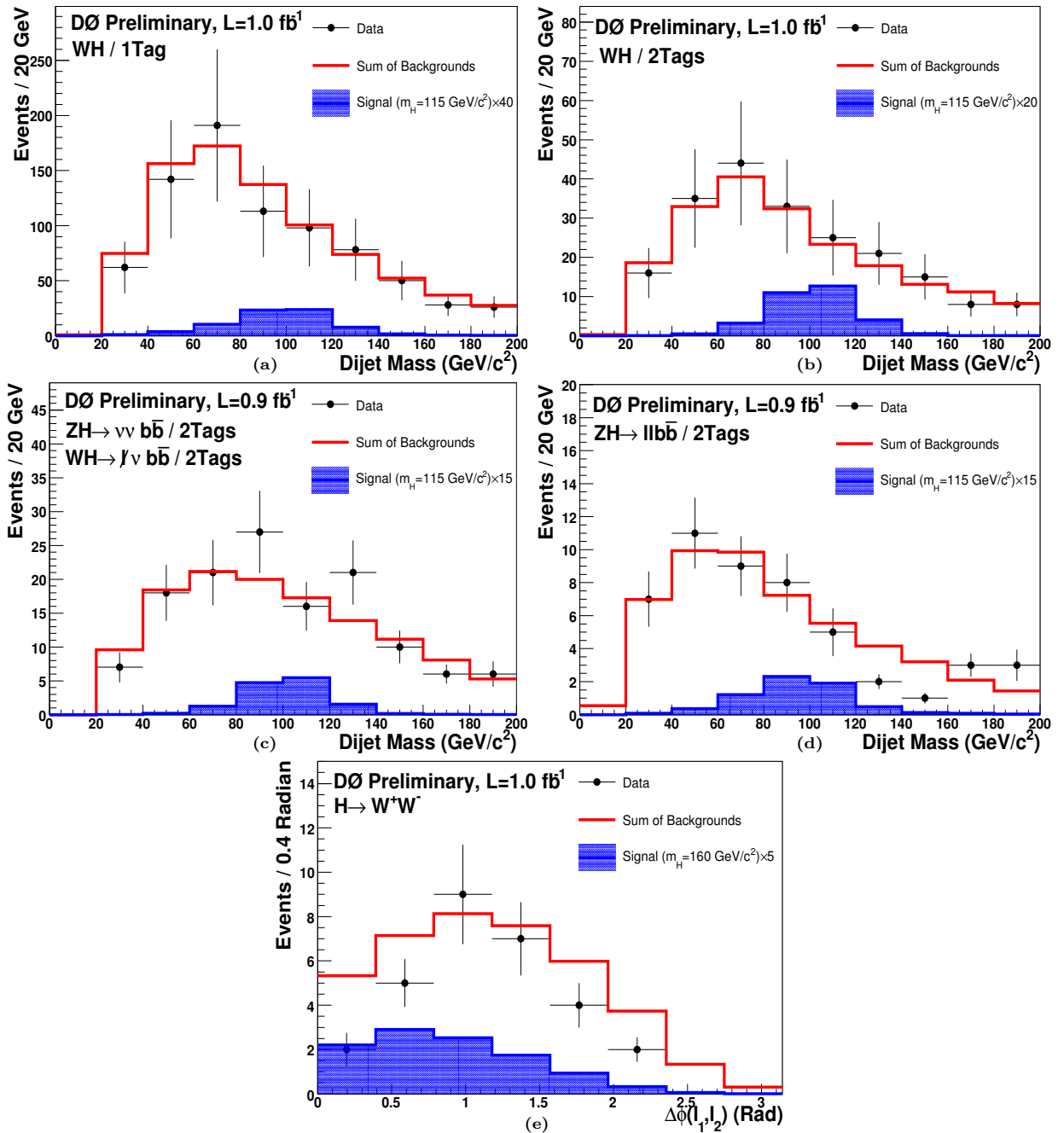


FIG. 1: Final variable distributions for selected Higgs search analyses. Shown in the figure are distributions for: the dijet invariant mass for  $WH \rightarrow e, \mu\nu b\bar{b}$  ST and DT analyses (a) and (b), the dijet invariant mass for the  $ZH \rightarrow \nu\bar{\nu}b\bar{b}$  DT analysis ( $ZH$  signal only) (c), the dijet invariant mass for the  $ZH \rightarrow \ell\bar{\ell}b\bar{b}$  DT analyses (d), and  $\Delta\varphi(\ell_1, \ell_2)$  for the  $H \rightarrow W^+W^-$  analyses (e). For all figures, background expectations and observed data are shown. The expected Higgs signals at selected masses are scaled as indicated.

### A. Results for Individual Channels

Figure 2 shows the expected LLR distributions for  $WH$ ,  $ZH$ , and  $H \rightarrow W^+W^-$  search channels, respectively. Included in these figures are the LLR values for the signal+background hypothesis ( $LLR_{s+b}$ ), background-only hypothesis ( $LLR_b$ ), and the observed data ( $LLR_{obs}$ ). The shaded bands represent the 1 and 2 standard deviation ( $\sigma$ ) departures for  $LLR_b$ . These distributions can be interpreted as follows:

TABLE II: List of leading correlated systematic uncertainties. The values for the systematic uncertainties are the same for the  $ZH \rightarrow \nu\bar{\nu}b\bar{b}$  and  $WH \rightarrow \ell\nu b\bar{b}$  channels. All uncertainties within a group are considered 100% correlated across channels. The correlated systematic uncertainty on the background cross section ( $\sigma$ ) is itself subdivided according to the different background processes in each analysis.

Source	$WH \rightarrow e\nu b\bar{b}$ DT(ST)	$WH \rightarrow \mu\nu b\bar{b}$ DT(ST)	$H \rightarrow W^+W^-$
Luminosity (%)	6.1	6.1	6.1
Jet Energy Scale (%)	5.0	5.0	3.0
Jet ID (%)	7.8	7.8	0
Electron ID (%)	6.7	0	2.3
Muon ID (%)	0	6.7	7.7
$b$ -Jet Tagging (%)	12.4(6.7)	8.5(5.0)	0
Background $\sigma$ (%)	6-18	6-18	6-18

Source	$ZH \rightarrow \nu\bar{\nu}b\bar{b}$	$ZH \rightarrow e^+e^-b\bar{b}$	$ZH \rightarrow \mu^+\mu^-b\bar{b}$
Luminosity (%)	6.1	6.1	6.1
Jet Energy Scale (%)	5.0	7.0	2.0
Jet ID (%)	7.1	7.0	5.0
Electron ID (%)	0	8.0	0
Muon ID (%)	0	0	12.0
$b$ -Jet Tagging (%)	9.6	12.0	22.0
Background $\sigma$ (%)	6-18	6-18	6-18

TABLE III: The correlation matrix for the analysis channels. The correlations for the  $ZH \rightarrow \nu\bar{\nu}b\bar{b}$  and  $WH \rightarrow \ell\nu b\bar{b}$  channels are held to be the same. All uncertainties within a group are considered 100% correlated across channels. The correlated systematic uncertainty on the background cross section ( $\sigma$ ) is itself subdivided according to the different background processes in each analysis.

Source	$WH \rightarrow e\nu b\bar{b}$	$WH \rightarrow \mu\nu b\bar{b}$	$ZH \rightarrow \nu\bar{\nu}b\bar{b}$	$ZH \rightarrow \ell\ell b\bar{b}$	$H \rightarrow W^+W^-$
Luminosity	×	×	×	×	
Jet Energy Scale	×	×	×	×	×
Jet ID	×	×	×	×	
Electron ID	×			×	×
Muon ID		×		×	×
$b$ -Jet Tagging	×	×	×	×	
Background $\sigma$	×	×	×	×	×

- The separation between  $LLR_b$  and  $LLR_{s+b}$  provides a measure of the discriminating power of the search. This is the ability of the analysis to separate the  $s + b$  and  $b$ -only hypotheses.
- The width of the  $LLR_b$  distribution (shown here as one and two standard deviation ( $\sigma$ ) bands) provides an estimate of how sensitive the analysis is to a signal-like fluctuation in data, taking account of the presence of systematic uncertainties. For example, when a  $1\text{-}\sigma$  background fluctuation is large compared to the signal expectation, the analysis sensitivity is thereby limited.
- The value of  $LLR_{obs}$  relative to  $LLR_{s+b}$  and  $LLR_b$  indicates whether the data distribution appears to be more signal-like or background-like. As noted above, the significance of any departures of  $LLR_{obs}$  from  $LLR_b$  can be evaluated by the width of the  $LLR_b$  distribution.

## B. Combined Results

The individual analyses described above can be grouped to form several combined limits:

- All  $WH$  searches (ST and DT) in the low mass range ( $m_H = 105 - 145 \text{ GeV}/c^2$ ).
- All  $ZH$  searches in the low mass range ( $m_H = 105 - 145 \text{ GeV}/c^2$ ).

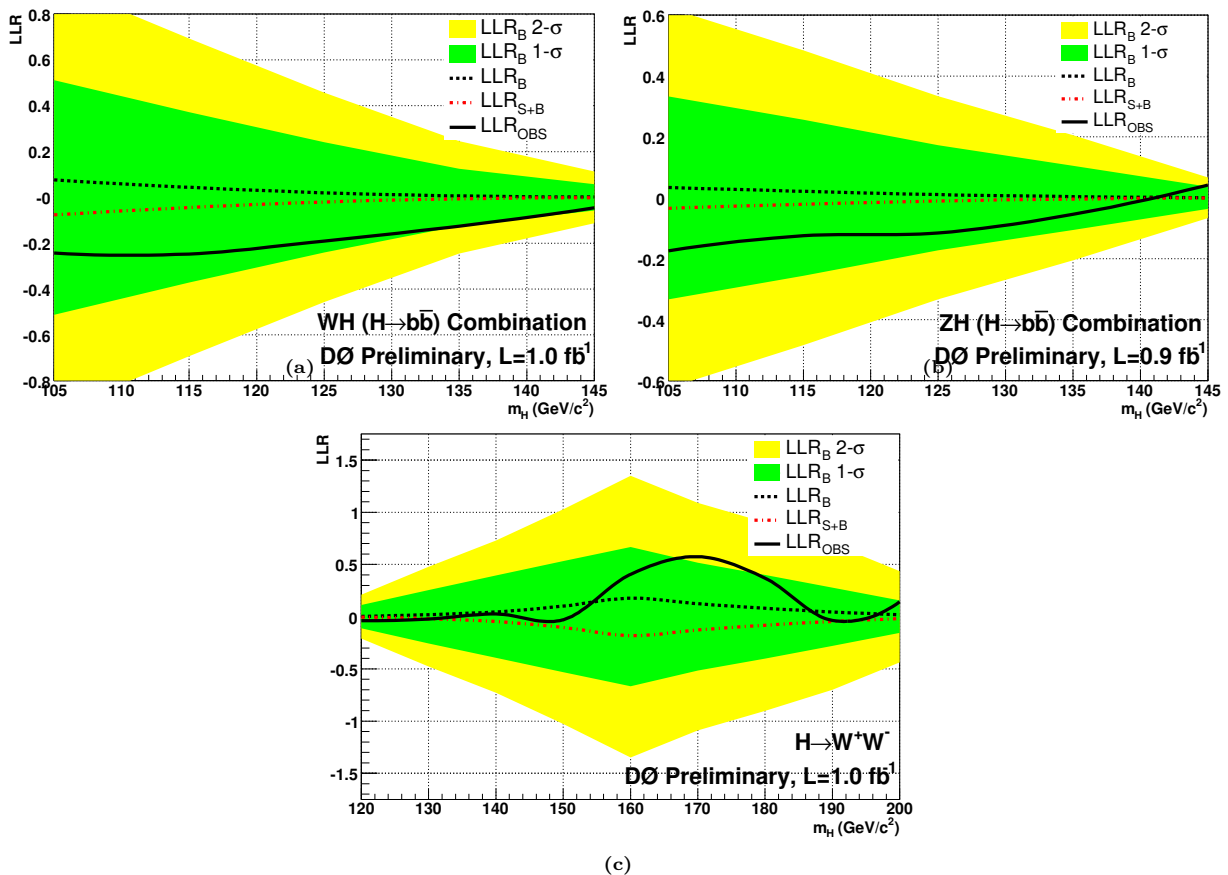


FIG. 2: Log-likelihood ratio distribution for the  $WH(H \rightarrow b\bar{b})$  analyses ( $WH \rightarrow e, \mu, \ell\nu b\bar{b}$ ) ST+DT final states combined (a), the  $ZH \rightarrow \ell\ell/\nu\nu b\bar{b}$  combined channels (b), and the  $H \rightarrow W^+W^-$  analyses ( $e^+e^-$ ,  $e^\pm\mu^\mp$ , and  $\mu^+\mu^-$  final states combined) (c).

- All  $WH$ ,  $ZH$  and  $H \rightarrow W^+W^-$  searches over the full mass range ( $m_H = 100 - 200 \text{ GeV}/c^2$ ).

Figures 3 and 4 show the expected and observed 95% CL cross section limit ratios for the combined  $WH$  analyses ( $WH \rightarrow e, \mu, \ell\nu b\bar{b}$  (ST+DT)) and the combined  $ZH$  analyses ( $ZH \rightarrow e^+e^-, \mu^+\mu^-, \nu\nu b\bar{b}$ ), respectively, in the mass range  $m_H = 105 - 145 \text{ GeV}/c^2$ . Figures 5 and 6 show the expected and observed 95% CL cross section limit ratios for all analyses combined in the low- and high-mass regions, respectively ( $m_H = 100 - 140 \text{ GeV}/c^2$  and  $m_H = 100 - 200 \text{ GeV}/c^2$ ). The LLR distribution for the full combination is shown in Fig. 7.

#### IV. CONCLUSIONS

We have presented results for eleven Higgs search analyses. We have combined these analyses to form new limits more sensitive than each individual limit.

- Combined observed (expected) 95% CL limit ratios to SM cross sections on  $p\bar{p} \rightarrow WH, H \rightarrow b\bar{b}$  range from 10.6 (8.1) at  $m_H = 115 \text{ GeV}/c^2$  to 29.3 (20.1) at  $m_H = 135 \text{ GeV}/c^2$ .
- Combined observed (expected) 95% CL limit ratios to SM cross sections on  $p\bar{p} \rightarrow ZH, H \rightarrow b\bar{b}$  range from 15.4 (12.2) at  $m_H = 115 \text{ GeV}/c^2$  to 34.3 (28.5) at  $m_H = 135 \text{ GeV}/c^2$ .
- Fully combined observed (expected) 95% CL limit ratios to SM cross sections on  $p\bar{p} \rightarrow WH/ZH/H, H \rightarrow b\bar{b}/W^+W^-$  range from 8.4 (5.9) at  $m_H = 115 \text{ GeV}/c^2$ , 3.7 (4.2) at  $m_H = 160 \text{ GeV}/c^2$ , and 13.5 (17.4) at  $m_H = 200 \text{ GeV}/c^2$ .

These relatively high cross section ratios will decrease strongly in the near future with the luminosity recorded at the Tevatron: more than  $2\text{fb}^{-1}$  is currently being analyzed and the Tevatron is expected to deliver  $8\text{fb}^{-1}$  by

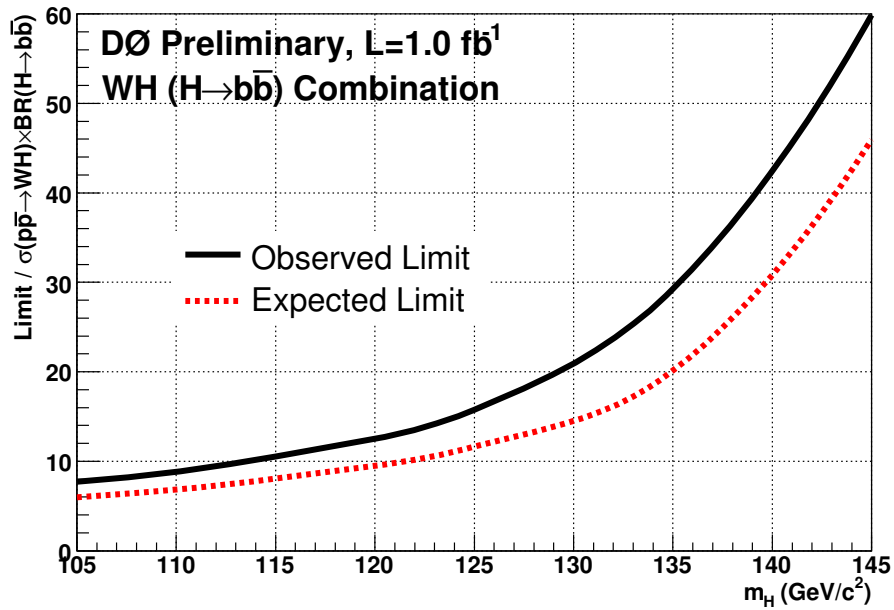


FIG. 3: Expected (median) and observed 95% CL cross section ratios for the combined  $WH$  analyses (ST/DT) in the  $m_H = 105 - 145$  GeV/c<sup>2</sup> mass range.

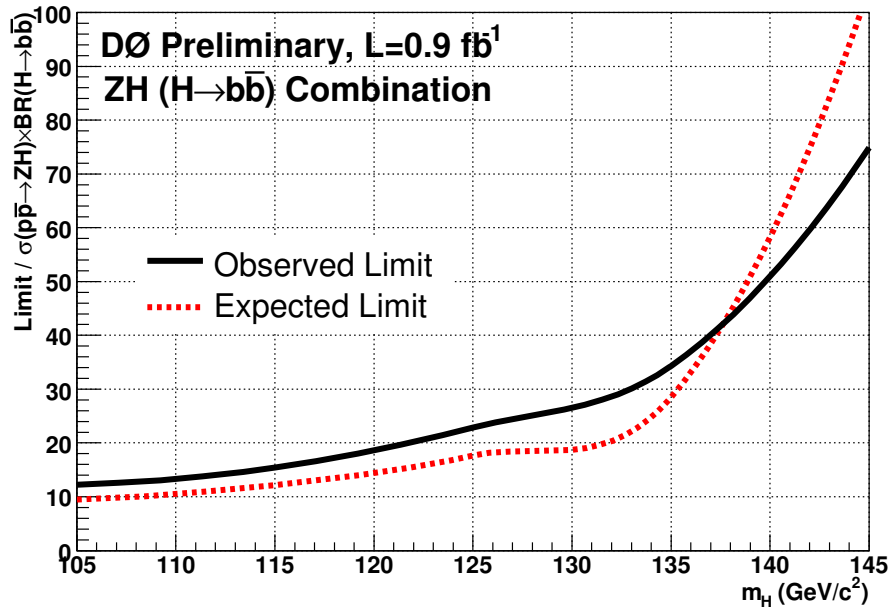


FIG. 4: Expected (median) and observed 95% CL cross section ratios for the combined  $ZH$  analyses in the  $m_H = 105 - 145$  GeV/c<sup>2</sup> mass range.

the end of 2009. Furthermore, we are developing new techniques to improve the current sensitivity: we expect improvements via multivariate analyses ( $\sim 30\%$  increase in sensitivity), and improved dijet mass resolution ( $\sim 25\%$  for  $m_H < 135$  GeV/c<sup>2</sup>). In addition, a forthcoming combination with the results from the CDF collaboration would yield an increase in sensitivity of  $\sim 40\%$ , as has been demonstrated previously [21].

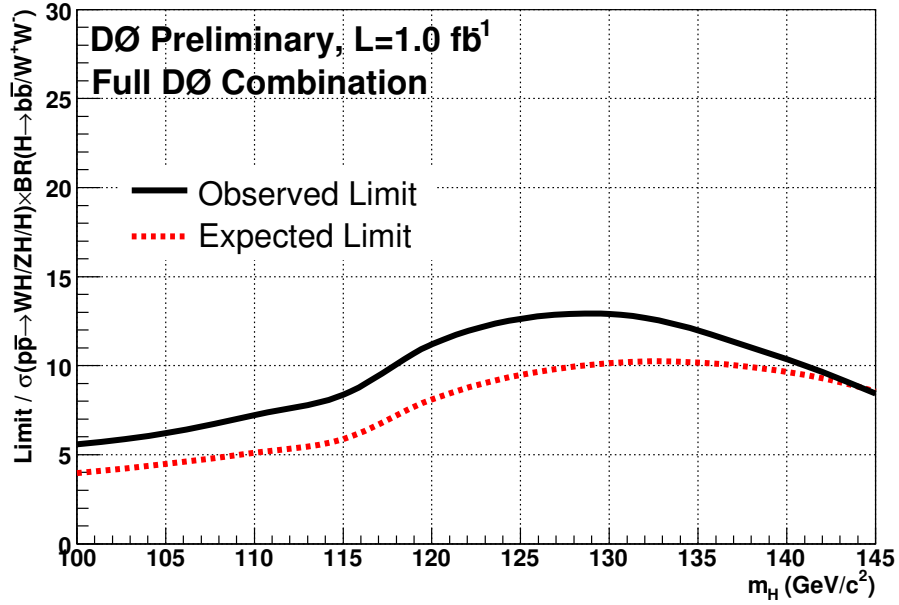


FIG. 5: Expected (median) and observed 95% CL cross section ratios for the combined  $WH/ZH/H, H \rightarrow b\bar{b}/W^+W^-$  analyses in the  $m_H = 100 - 145 \text{ GeV}/c^2$  mass range.

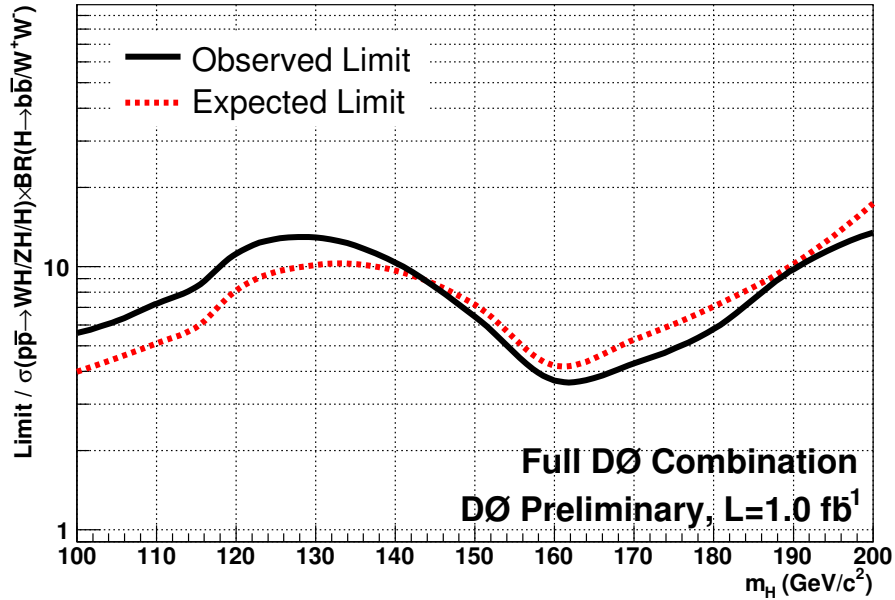


FIG. 6: Expected (median) and observed 95% CL cross section ratios for the combined  $WH/ZH/H, H \rightarrow b\bar{b}/W^+W^-$  analyses in the  $m_H = 100 - 200 \text{ GeV}/c^2$  mass range.

#### Acknowledgments

We thank the staffs at Fermilab and collaborating institutions, and acknowledge support from the DOE and NSF (USA); CEA and CNRS/IN2P3 (France); FASI, Rosatom and RFBR (Russia); CAPES, CNPq, FAPERJ, FAPESP and FUNDUNESP (Brazil); DAE and DST (India); Colciencias (Colombia); CONACyT (Mexico); KRF and KOSEF (Korea); CONICET and UBACyT (Argentina); FOM (The Netherlands); PPARC (United Kingdom); MSMT (Czech Republic); CRC Program, CFI, NSERC and WestGrid Project (Canada); BMBF and DFG (Germany); SFI (Ireland);

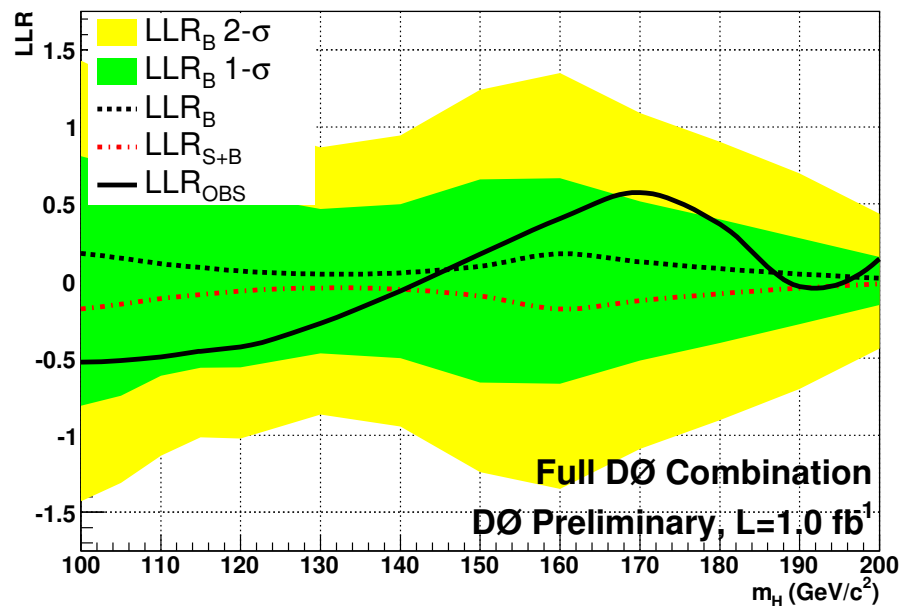


FIG. 7: Log-likelihood ratio distribution for the combined  $WH/ZH/H, H \rightarrow b\bar{b}/W^+W^-$  analyses in the  $m_H = 100 - 200 \text{ GeV}/c^2$  mass range.

Research Corporation, Alexander von Humboldt Foundation, and the Marie Curie Program.

- 
- [1] R. Barate *et al.* [LEP Working Group for Higgs boson searches], Phys. Lett. B **565**, 61 (2003), [arXiv:hep-ex/0306033].
- [2] LEP Electroweak Working Group: <http://lepewwg.web.cern.ch/LEPEWWG/> (March 2007 update <http://lepewwg.web.cern.ch/LEPEWWG/plots/winter2007/>).
- [3] DØ Collaboration, V. Abazov *et al.*, “The Upgraded DØ Detector”, Nucl. Instrum. Meth. A **565**, 463 (2006), [arXiv:hep-ex/0507191].
- [4] DØ Collaboration, “Search for WH production at  $\sqrt{s} = 1.96 \text{ TeV}$  with  $1 \text{ fb}^{-1}$  of Data,” DØ Conference Note 5357.
- [5] DØ Collaboration, “A Search for Standard Model Higgs Boson in the Channel  $ZH \rightarrow \nu\bar{\nu}b\bar{b}$  at  $\sqrt{s} = 1.96 \text{ TeV}$  at DØ,” DØ Conference Note 5353.
- [6] DØ Collaboration, “A Search for  $ZH \rightarrow \ell\bar{\ell}b\bar{b}$  Production at DØ with  $0.84\text{-}0.92 \text{ fb}^{-1}$  Integrated Luminosity,” DØ Conference Note 5275.
- [7] DØ Collaboration, “Search for the Higgs boson in  $H \rightarrow WW^* \rightarrow l^+l^- (ee, e\mu)$  decays with  $950 \text{ pb}^{-1}$  at DØ in Run II,” DØ Conference Note 5063.
- [8] DØ Collaboration, “Search for the Higgs boson in  $H \rightarrow WW^* \rightarrow \mu\mu$  decays with  $930 \text{ pb}^{-1}$  at DØ in Run II,” DØ Conference Note 5194.
- [9] T. Sjöstrand, P. Edén, C. Friberg, L. Lönnblad, G. Miu, S. Mrenna and E. Norrbin, Comput. Phys. Commun. **135** (2001) 238 (LU TP 00-30, [arXiv:hep-ph/0010017]).
- [10] J. Pumplin *et al.*, “New Generation of Parton Distributions with Uncertainties from Global QCD Analysis”, JHEP 0207(2002)012 doi:10.1088/1126-6708/2002/07/012.
- [11] S. Catani *et al.*, “Soft-gluon resummation for Higgs boson production at hadron colliders,” JHEP **0307**, 028 (2003), [arXiv:hep-ph/0306211].
- [12] K. A. Assamagan *et al.* [Higgs Working Group Collaboration], “The Higgs working group: Summary report 2003,” [arXiv:hep-ph/0406152].
- [13] A. Djouadi, J. Kalinowski and M. Spira, “HDECAY: A program for Higgs boson decays in the standard model and its supersymmetric extension,” Comput. Phys. Commun. **108**, 56 (1998) [arXiv:hep-ph/9704448].
- [14] M. L. Mangano *et al.*, “ALPGEN, a generator for hard multiparton processes in hadronic collisions,” JHEP **0307**, 001 (2003) [arXiv:hep-ph/0206293].
- [15] A. Pukhov *et al.*, “CompHEP: A package for evaluation of Feynman diagrams and integration over multi-particle phase space. User’s manual for version 33,” [arXiv:hep-ph/9908288].
- [16] J. Campbell and R. K. Ellis, “Next-to-leading order corrections to  $W + 2\text{jet}$  and  $Z + 2\text{jet}$  production at hadron colliders,” Phys. Rev. D **65**, 113007 (2002), [arXiv:hep-ph/0202176].
- [17] T. Junk, Nucl. Instrum. Meth. A **434**, 435-443 (1999). Alex Read, “Modified Frequentist Analysis of Search Results (The

- CLs Method)” CERN 2000-005 (30 May 2000).
- [18] K. S. Cranmer, *Comput. Phys. Commun.*, **136**, 198 (2001), [arXiv:hep-ph/0011057].
  - [19] A. Read, *NIM A* 425 357-360 (1999).
  - [20] W. Fisher, “Systematics and Limit Calculations,” FERMILAB-TM-2386-E.
  - [21] CDF and DØ Collaborations, “Combined DØ and CDF Upper Limits on Standard-Model Higgs-Boson Production,” CDF Note 8384, DØ Note 5227.